

Article

An Experimental Study of Two-Phase Pulse Flushing Technology in Water Distribution Systems

Zhaozhao Tang ¹, Wenyan Wu ² , Xiaoxi Han ³ and Ming Zhao ^{3,*}

¹ School of Computing and Digital Technologies, Staffordshire University, Stoke on Trent ST4 2DE, UK; zhaozhao.tang@foxmail.com

² School of Engineering and the Built Environment, Birmingham City University, Birmingham B4 7XG, UK; wenyan.wu@bcu.ac.uk

³ School of Municipal and Environmental Engineering, Harbin Institute of Technology, Harbin 150090, China; h9090@foxmail.com

* Correspondence: zhming1188@126.com; Tel.: +86-451-8628-2332

Received: 17 October 2017; Accepted: 21 November 2017; Published: 28 November 2017

Abstract: The deterioration of drinking water during distribution process is caused by many factors. The microorganisms and substances peeling off from the “growth-ring” make the secondary pollution in drinking water distribution systems. To reduce the secondary pollution, two-phase pulse flushing technology is introduced to quickly remove the “growth-ring”. In this study, experiment is undertaken for investigating the efficiency of the two-phase pulse flushing and finding the best setting combination. A case study is undertaken to compare the efficiencies between the two-phase pulse and the single-phase flushing. The best setting combination of the two-phase pulse flushing is at the frequency 4 s–6 s (air inflow time is 4 s and air cut off time is 6 s) and the round air inflow nozzle is set at the bottom of the pipe. Two-phase pulse flushing technology can save 95% of water and 6 h 40 min flushing time.

Keywords: water distribution system; secondary pollution; growth-ring; flushing

1. Introduction

The water consumed by the consumers travels large distances and takes long durations through the water distribution system. The secondary pollution causing deterioration occurs after clean drinking water leaves the treatment plant. The deterioration in drinking water quality is influenced by many factors, e.g., decay of disinfectant residual, temperature, hydraulic regime, water residence time, bacterial regrowth, etc. [1–3].

During drinking water distribution, the secondary pollution is mainly caused by the so-called “growth-ring”. Sediments attach on the pipe wall, and they can interact with the pipe wall materials by chemical or electrochemical processes and microorganisms, which forms an irregular “growth-ring” towards the centre of the pipe [4–7]. The microorganisms and substances peeling off from the “growth-ring” into bulk water is the main mechanism of the secondary pollution in drinking water distribution system [8].

The “growth-ring” contains high percentage of water which takes generally over 1/3 and sometimes even over 1/2 of the contents [4]. Through X-ray diffraction (XRD) and X-ray photoelectron spectroscopy (XPS) analysis, the main ingredients of the “growth-ring” are goethite, ferrous sulphide, etc., while iron is the major element, approximately 55% of the content [4]. The “growth-ring” generally has three layers: biological membrane layer, deposition layer and corrosion layer. This structure provides the environment for the growth of bacteria, and the bacteria can promote the corrosion of the metal [9]. Sanitisers are used to control the growth of microorganisms, but residual sanitisers can increase the reaction velocity of corrosion [10]. The “growth-ring” can also cause leakage because its

growth occupies the room for water distribution. Therefore, it is imperative to reduce the influence of the “growth-ring” in order to improve the drinking water quality.

This paper experimentally investigates the two-phase pulse flushing technology for efficient removal of the “growth-ring”. The influences of different pulse frequencies, shapes of inlets and locations of the inlets are discussed in order to obtain the best setting combination. A case study of the comparison between two-phase pulse and single-phase flushing is presented in this paper.

2. Two-Phase Pulse Flushing Experiment

2.1. Experiment Set Up

The experiment set up scheme is shown in Figure 1, and Figure 2 is the practical experiment set up in the lab. The material of the pipes used for this experiment is polymethyl methacrylate. The pipes are connected by flanges. The internal diameter of the pipes is 40 mm, and the external diameter is 60 mm. The size of the water tank is 2000 mm × 2000 mm × 1000 mm. The framework consists of a circulatory water supply system, an air supply system, an experimental pipe line with feeding device and a data acquisition system.

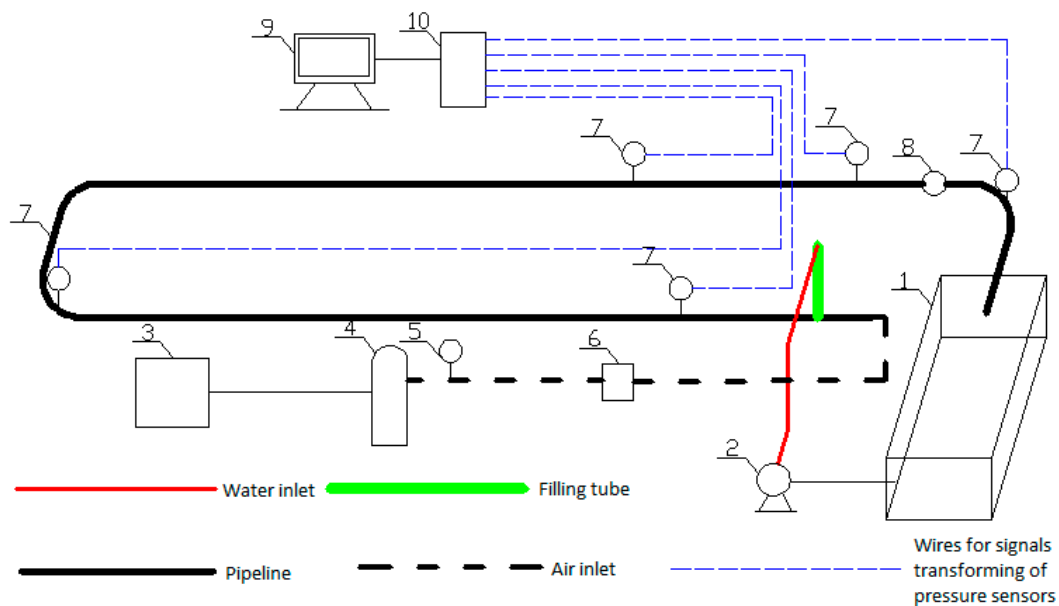


Figure 1. Two-phase pulse flushing experiment set up: (1) water tank; (2) water pump; (3) wire compressor; (4) gasholder; (5) pressure control valve; (6) pulse generator; (7) pressure transmitter; (8) flow meter; (9) computer; and (10) data acquisition module.

The water pump draws the water from the water tank and the flow rate is controlled by the valve. The measurement of the flow rate is undertaken by the flow meter. Air goes into the air compressor for compressing. Air pressure is controlled by the gasholder. In this two-phase (gas and water) experiment set up, the entire pipeline is strictly sealed. The pumped-out water and the compressed air are mixed in a T joint and then flow into the water tank along the pipeline. In the end, the water flows into the water tank for circulatory use.



Figure 2. Practical two-phase pulse flushing experiment set up in the laboratory.

2.2. Single-Phase Flushing

A single-phase flushing investigation is undertaken for comparison with the following two-phase pulse flushing with different settings. Air flow is closed and only water flows into the pipeline. The average water flow rate is $0.0026 \text{ m}^3/\text{s}$, and the velocity of the water flow is 2.07 m/s . The average pressure head at pressure sensing locations No. 1, 2, 3, 4 and 5, according to Figure 1, are 2.19 m (metres of water), 1.83 m , 1.79 m , 1.59 m and 0.74 m , respectively. Under the conditions of identical temperature values, pipe materials and diameters, if the flow velocity is greater than the critical value 0.066 m/s , the water flow in the pipeline is turbulent (Reynolds number $Re > Re_c = 2300$).

2.3. Two-Phase Pulse Flushing

In this research, the air inflow and cut off time is from 3 to 6 s. Different shapes of nozzles (round, rectangular and slot) and different locations of nozzles (in the middle, on top or on bottom of the pipe) are set for experimental results comparison.

The experiment is undertaken by only changing one of the conditions (air inflow and cut off time, nozzle shape and location). The best condition combination is obtained by following the following principles. Setting the nozzle shape and location invariant, the pressure fluctuation of No. 1 pressure sensing point is recorded as the prioritised reference, and the average flow velocity is recorded as the subordinate reference. The best air inflow frequency is obtained when the pressure fluctuation reaches maximum and the flow velocity reaches a high value simultaneously. If the flow velocity does not reach a high value at the maximum pressure fluctuation point, it needs to be evaluated at the second, third, etc. highest pressure fluctuation point until the flow velocity reaches a high value. The best air inflow frequency can be obtained by using the rules above.

2.3.1. Round Nozzle

In the Middle of the Pipe

Setting the air inflow time invariant, Figure 3 shows the maximum average peak pressure of the flow inside the pipe comes after the air inflow is cut off for 6 s. The average peak pressure is 8.1 m when the frequency is 4 s–6 s (air inflow time 4 s and air cut off time 6 s). When the frequency is 5 s–6 s and 6 s–6 s, the average peak pressure is 8.96 m and 7.94 m, respectively. Figure 4 shows the pressure comparison of the four best frequencies. When air cut off duration is 6 s, few differences are caused by pulse frequency through applying different air inflow time. The result shows that the peak pressure reaches the maximum 8.96 m at the frequency 5 s–6 s (round nozzle in the middle of the pipe).

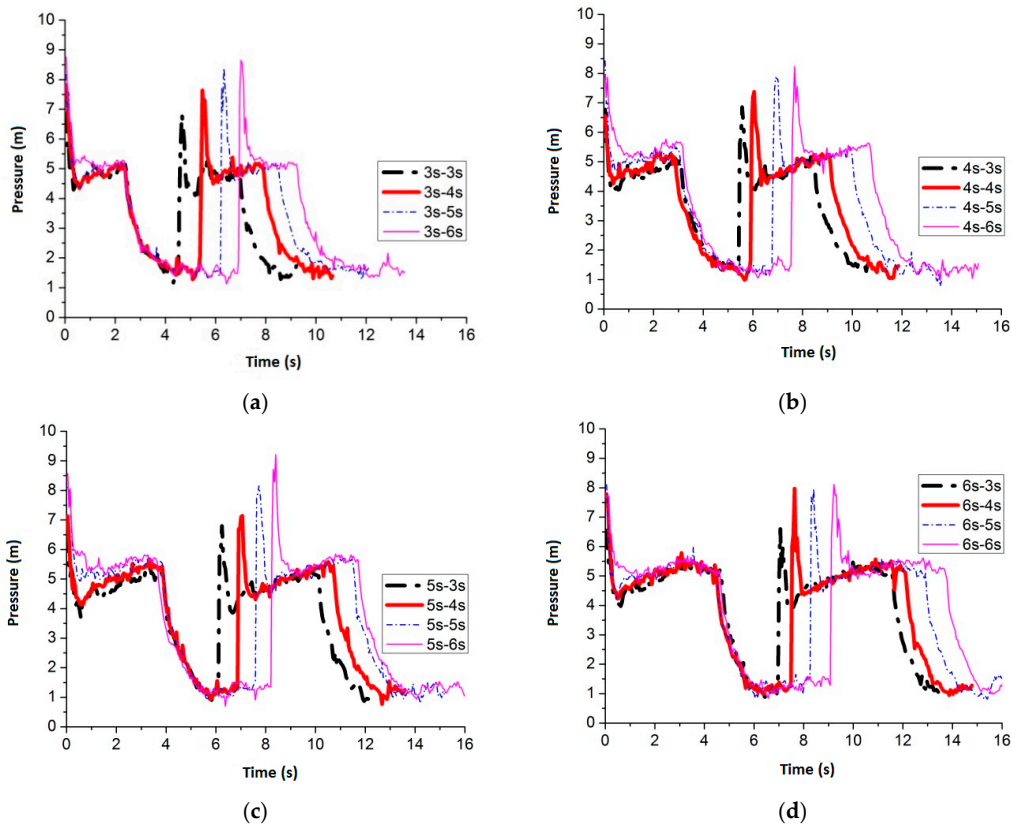


Figure 3. Pressure fluctuation of No. 1 sensing point (round nozzle is in the middle of the pipe): (a) air inflow time is 3 s; (b) air inflow time is 4 s; (c) air inflow time is 5 s; and (d) air inflow time is 6 s.

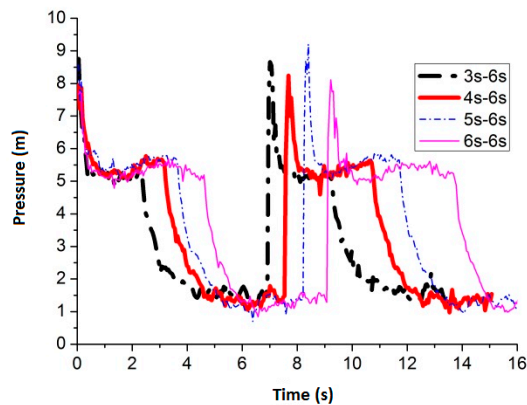


Figure 4. The four best pressure values (round nozzle in the middle of the pipe).

The best frequency is not clear after air inflow is cut off for 6 s through the comparison of the four best pressure values in Figure 4. Therefore, four cycles of pressure data are selected to perform the statistical analysis in every operating condition to help find the best frequency (Table 1).

Table 1. Pressure values and statistical analysis after air inflow has been cut off for 6 s (round nozzle in the middle of the pipe).

Parameter Frequency	Average Peak Value (m)	Average Minimum Value (m)	Variation Range (m)	Average Value (m)	Peak Value Deviation
3 s–6 s	8.6307	1.2199	7.4108	3.1813	0.0762
4 s–6 s	8.6887	0.9891	7.6997	3.4123	0.2182
5 s–6 s	8.7165	0.7111	8.0055	3.5498	0.2466
6 s–6 s	7.8426	0.8766	6.9660	3.5534	0.1348

Figure 5 shows the average flow velocity of the water flow in the pipe by applying above settings.

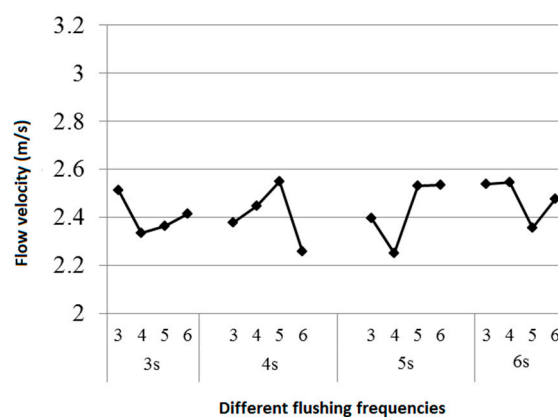


Figure 5. Comparison of water flow velocity at all frequencies (round nozzle in the middle of the pipe).

In Table 1 and Figure 5, the best frequency for the round nozzle in the middle of the pipe can be obtained as 5 s–6 s. The average water flow velocity can reach 2.534 m/s in the pipe at the frequency 5 s–6 s. Although the pressure peak value deviation at 5 s–6 s is slightly higher than the other three frequencies, the average peak pressure value and the fluctuation range reach maximum simultaneously.

Nozzle on Top of the Pipe

Figure 6 shows the maximum average peak pressure comes after air inflow is cut off for 6 s by setting the air inflow time invariant. When the frequency is 3 s–6 s, 4 s–6 s, 5 s–6 s and 6 s–6 s, the average peak pressure reaches 8.20 m, 8.31 m, 8.47 m and 8.08 m, respectively. Figure 7 shows the pressure comparison of the four best frequencies. When air cut off duration is 6 s, few differences are caused by pulse frequency through applying different air inflow time. The result shows that the peak pressure reaches the maximum 8.47 m at the frequency 5 s–6 s (round nozzle on top of the pipe).

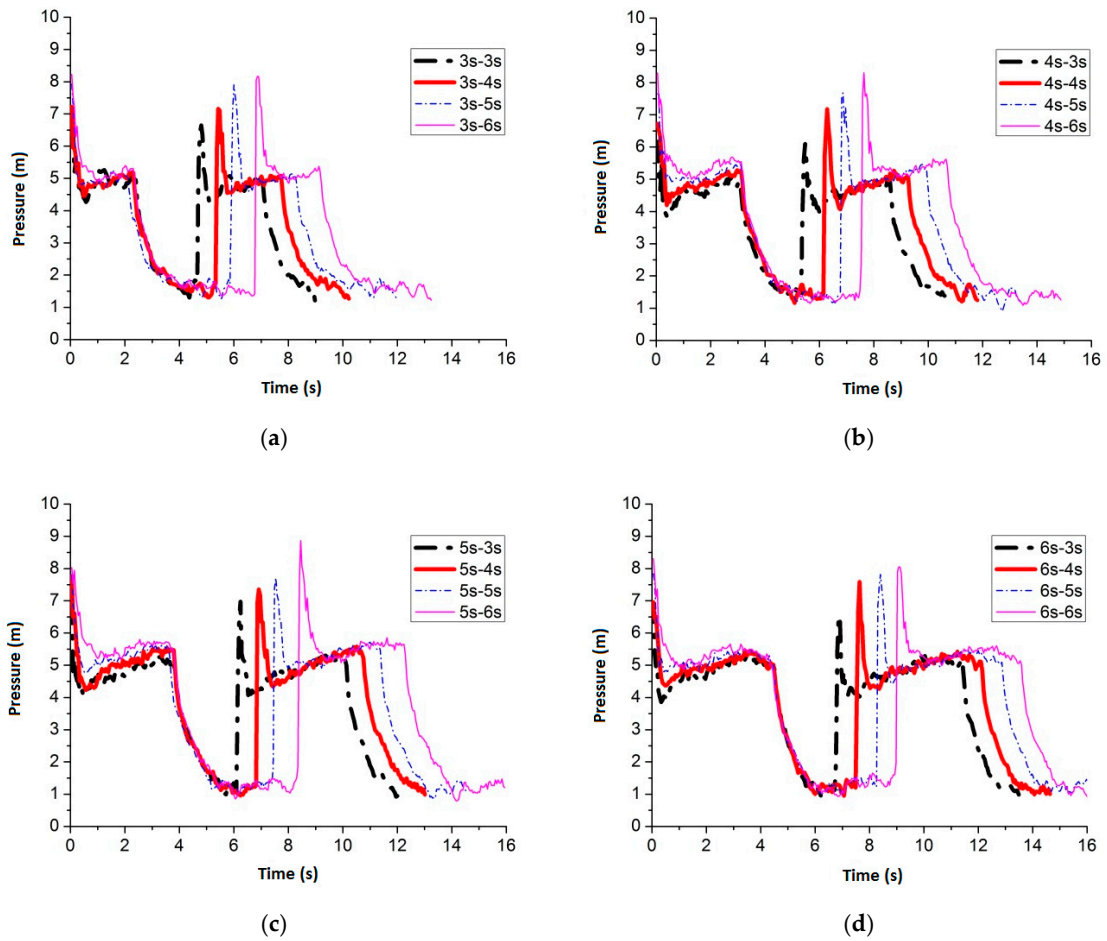


Figure 6. Pressure fluctuation of No. 1 sensing point (round nozzle on top of the pipe): (a) air inflow time is 3 s; (b) air inflow time is 4 s; (c) air inflow time is 5 s; and (d) air inflow time is 6 s.

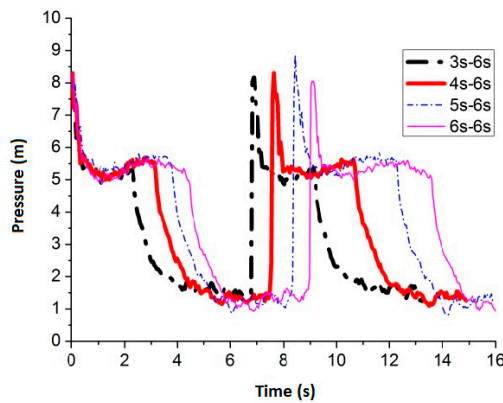


Figure 7. The four best pressure values (round nozzle on top of the pipe).

The best frequency is not clear after air inflow is cut off for 6 s through the comparison of the four best pressure values in Figure 7. Therefore, four cycles of pressure data are selected to perform the statistical analysis in every operating condition to help find the best frequency (Table 2).

Table 2. Pressure values and statistical analysis after air inflow has been cut off for 6 s (round nozzle on top of the pipe).

Frequency	Parameter	Average Peak Value (m)	Average Minimum Value (m)	Variation Range (m)	Average Value (m)	Peak Value Deviation
3 s–6 s		8.3974	1.1897	7.2077	3.1624	0.2393
4 s–6 s		8.6875	1.0217	7.6658	3.3755	0.2635
5 s–6 s		8.3382	0.8235	7.5174	3.5776	0.2913
6 s–6 s		8.1146	0.8476	7.2669	3.5676	0.0955

Figure 8 shows the average flow velocity of the water flow in the pipe by applying above settings.

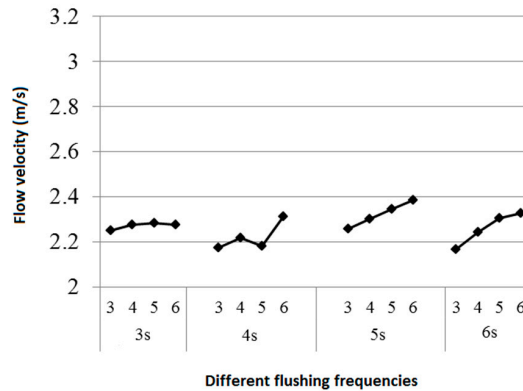


Figure 8. Comparison of water flow velocity at all frequencies (round nozzle on top of the pipe).

In Table 2 and Figure 8, the best frequency can be obtained as 4 s–6 s (round nozzle on top of the pipe). The average peak pressure value and the fluctuation range of No. 1 sensing point reach maximum simultaneously and the average water flow velocity reaches a high value 2.311 m/s in the pipe at the frequency 4 s–6 s.

Nozzle at the Bottom of the Pipe

Figure 9 shows the maximum average peak pressure comes after air inflow is cut off for 6 s by setting the air inflow time invariant. When the frequency is 3 s–6 s, 4 s–6 s, 5 s–6 s and 6 s–6 s, the average peak pressure is 8.74 m, 9.03 m, 8.00 m and 7.88 m, respectively. Figure 10 shows the pressure comparison of the four best frequencies. Few differences are caused by pulse frequency by applying different air inflow time after air inflow is cut off for 6 s. When the frequency is 4 s–6 s, the peak pressure reaches the maximum value 9.03 m (round nozzle at the bottom of the pipe).

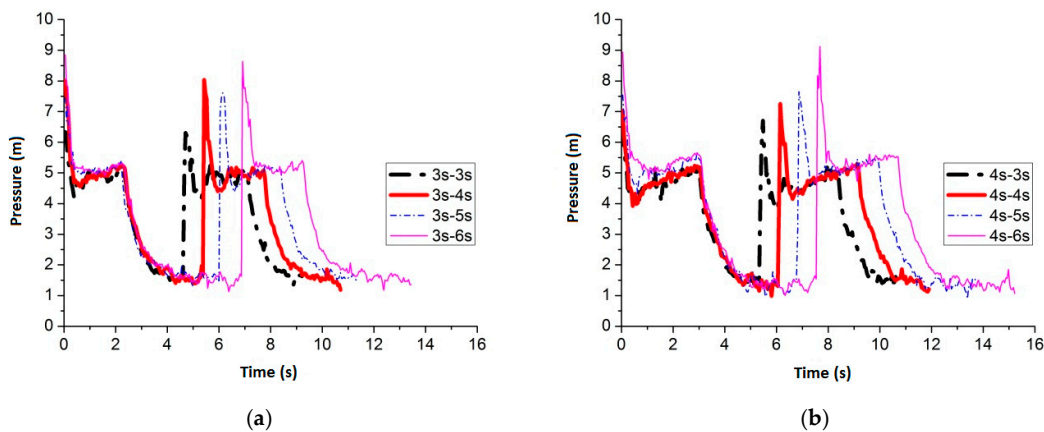


Figure 9. Cont.

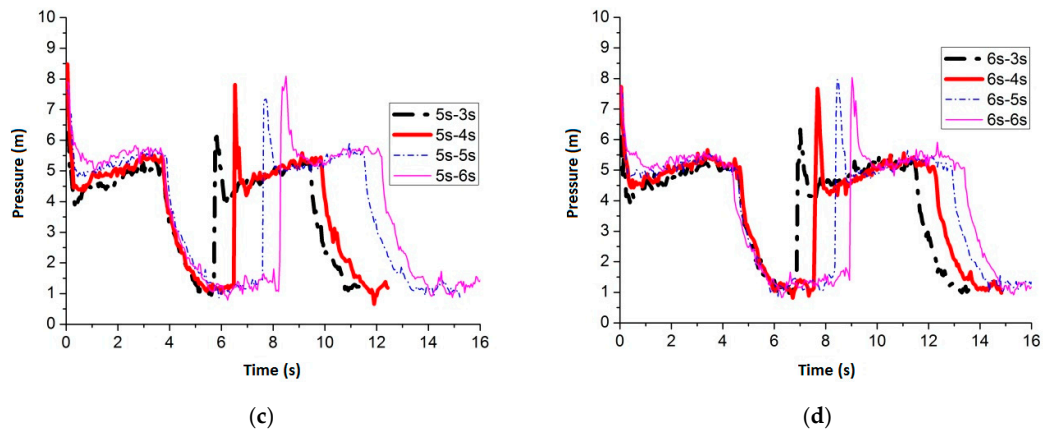


Figure 9. Pressure fluctuation of No. 1 sensing point (round nozzle at the bottom of the pipe): (a) air inflow time is 3 s; (b) air inflow time is 4 s; (c) air inflow time is 5 s; and (d) air inflow time is 6 s.

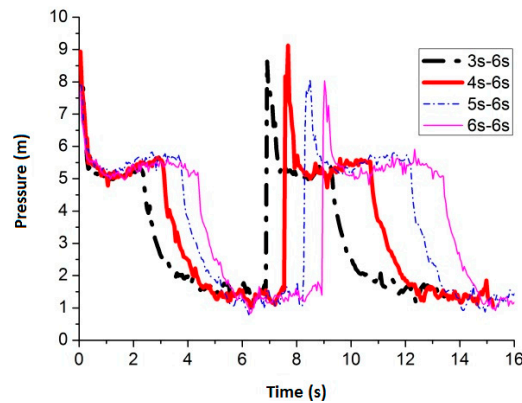


Figure 10. The four best pressure values (round nozzle at the bottom of the pipe).

The best frequency is not clear after air inflow is cut off for 6 s through the comparison of the four best frequencies (Figure 10). Therefore, four cycles of pressure data are selected to perform the statistical analysis in every operating condition to help find the best frequency (Table 3).

Table 3. Pressure values and statistical analysis after air inflow has been cut off for 6 s (round nozzle at the bottom of the pipe).

Frequency	Parameter	Average Peak Value (m)	Average Minimum Value (m)	Variation Range (m)	Average Value (m)	Peak Value Deviation
3 s–6 s		8.7697	1.1305	7.6392	3.2263	0.2949
4 s–6 s		8.9498	1.0193	7.9305	3.4144	0.1342
5 s–6 s		8.2246	0.7642	7.4603	3.5700	0.1704
6 s–6 s		7.8571	0.8174	7.0397	3.5493	0.1583

Figure 11 shows the average flow velocity of the water flow in the pipe by applying the above flushing conditions.

In Table 3 and Figure 11, the best frequency can be obtained as 4 s–6 s (round nozzle at the bottom of the pipe). The average peak pressure value and the fluctuation range of No. 1 sensing point reach maximum simultaneously and the average water flow velocity reaches a high value 2.957 m/s at the frequency 4 s–6 s.

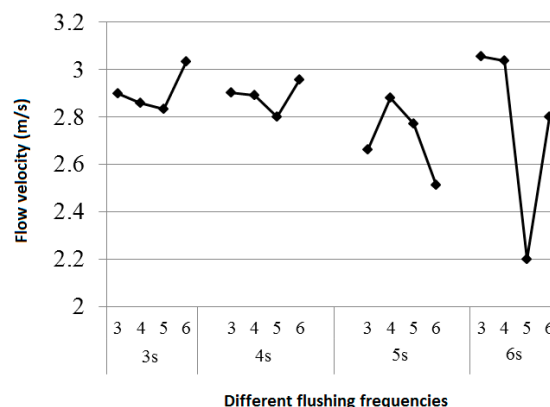


Figure 11. Flow velocity comparison of all frequencies (round nozzle at the bottom of the pipe).

Comparison of Nozzle Locations

At the best flushing frequencies, by using the same nozzle shape (round) and setting different nozzle locations, the fluctuation range and the flow velocity of No. 1 sensing point are compared and given in Table 4. Setting the round nozzle on top of the pipe, the peak pressure and the average flow velocity reach maximum simultaneously, the peak value deviation reaches minimum, and the fluctuation range is high. The above results indicate that the best and most reliable choice for flushing is to set the nozzle at the bottom of the pipe and process at the best frequencies. The best frequency is 4 s–6 s or 5 s–6 s. The best air inflow frequency not only ensures enough air inflow quantity for keeping the ejection flow flushing, but also avoids the negative effects on the flushing results by over air inflow amount. Two-phase (gas and water) high energy flushing effect on the internal pipe wall can be secured at the best air inflow frequencies.

Table 4. Flushing results by setting round nozzle at different locations.

Location	Parameter	Average Peak Value (m)	Average Minimum Value (m)	Variation Range (m)	Average Value (m)	Peak Value Deviation	Flow Velocity (m/s)
Top (4 s–6 s)		8.6875	1.0217	7.6658	3.3755	0.2635	2.311
Middle (5 s–6 s)		8.7165	0.7111	8.0055	3.5498	0.2466	2.534
Bottom (4 s–6 s)		8.9498	1.0193	7.9305	3.4144	0.1342	2.957

2.3.2. Rectangular Nozzle

Nozzle in the Middle of the Pipe

Figure 12 shows similar regularity as the former results. The static peak pressure on top of the internal pipe increases with the increase of the air inflow cut off time. The pressure saltation becomes more obvious with the increase of the air inflow cut off time, and therefore turbulence increases, which promotes the cleaning for the pipelines. The maximum average peak pressure comes after air inflow is cut off for 6 s by setting air inflow time invariant. When the frequency is 3 s–6 s, 4 s–6 s, 5 s–6 s and 6 s–6 s, the average peak pressure is 8.21 m, 7.98 m, 8.10 m and 8.00 m, respectively. Figure 13 shows the pressure comparison of the four best frequencies. When air cut off duration is 6 s, few differences are caused by pulse frequency by applying different air inflow time. At the frequency 3 s–6 s, the peak pressure value reaches maximum, which is 8.21 m (rectangular nozzle in the middle of the pipe).

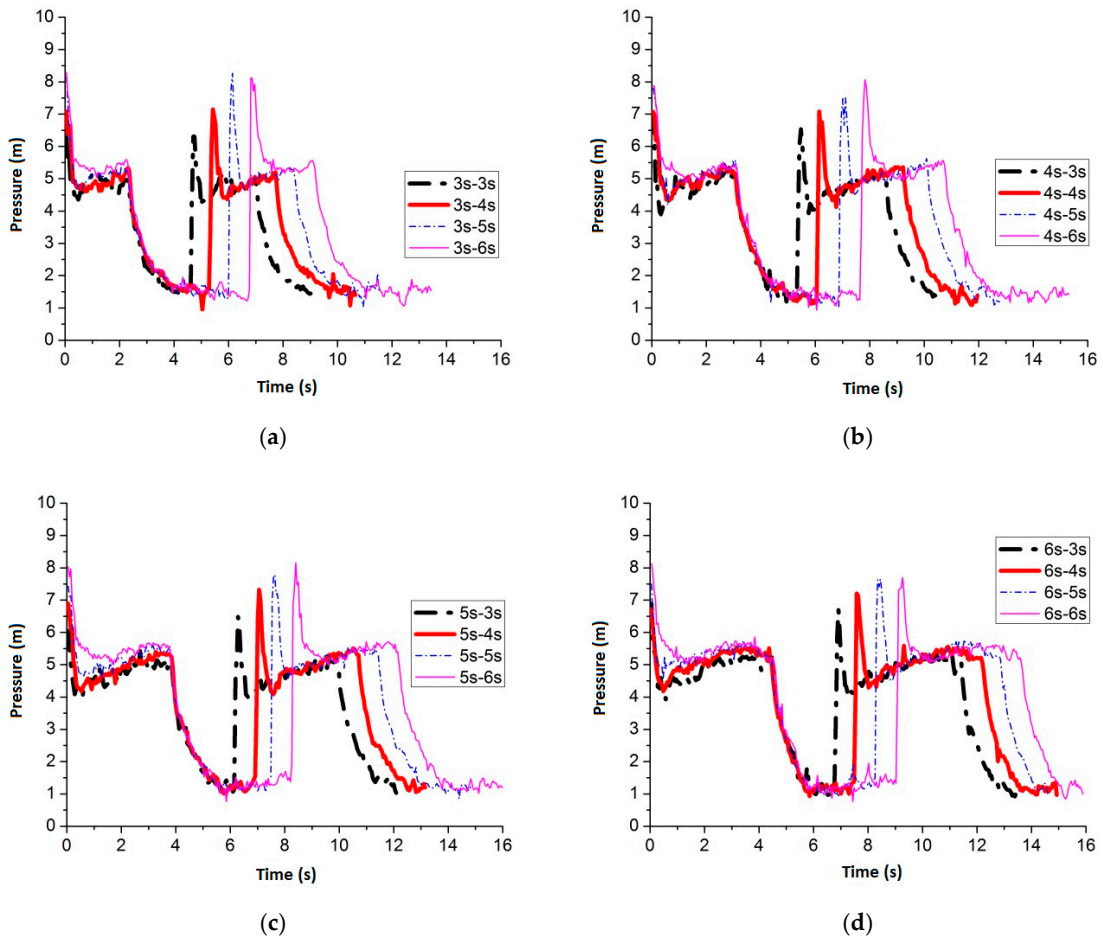


Figure 12. Pressure fluctuation of No. 1 sensing point (rectangular nozzle in the middle of the pipe): (a) air inflow time is 3 s; (b) air inflow time is 4 s; (c) air inflow time is 5 s; and (d) air inflow time is 6 s.

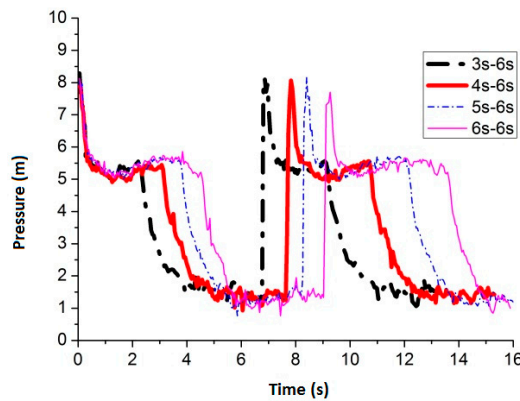


Figure 13. The four best pressure values (rectangular nozzle in the middle of the pipe).

The best frequency is not clear after air inflow is cut off for 6 s through the comparison of the four best frequencies (Figure 13). Therefore, four cycles of pressure data are selected to perform the statistical analysis in every operating condition to help find the best frequency (Table 5).

Table 5. Pressure values and statistical analysis after air inflow has been cut off for 6 s (rectangular nozzle in the middle of the pipe).

Frequency \ Parameter	Average Peak Value (m)	Average Minimum Value (m)	Variation Range (m)	Average Value (m)	Peak Value Deviation
3 s–6 s	8.3926	1.0700	7.3225	3.2356	0.3094
4 s–6 s	8.2113	1.0048	7.2065	3.3311	0.4025
5 s–6 s	8.3588	0.8404	7.5184	3.4978	0.2635
6 s–6 s	8.4591	0.8235	7.6356	3.6207	0.1342

Figure 14 shows the average flow velocity of the water flow in the pipe by applying the above flushing conditions.

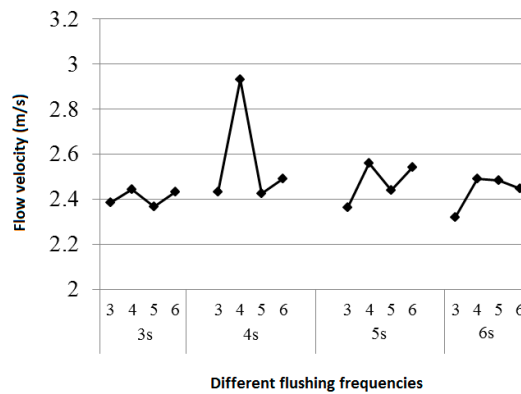


Figure 14. Flow velocity comparison of all the frequencies when the rectangular nozzle is in the middle.

In Table 5 and Figure 14, the best frequency can be obtained as 6 s–6 s (rectangular nozzle in the middle of the pipe). The average water flow velocity reaches 2.447 m/s in the pipe at the frequency 6 s–6 s, and the average peak pressure value and the fluctuation range reach maximum simultaneously.

Nozzle on Top of the Pipe

Figure 15 shows that the static pressure peak value on top of the internal pipe wall increases with the increase of the air inflow cut off time. The maximum average peak pressure comes after air inflow is cut off for 6 s by setting air inflow time invariant. When the frequency is 3 s–6 s, 4 s–6 s, 5 s–6 s and 6 s–6 s, the average peak pressure is 8.32 m, 8.13 m, 8.45 m and 7.81 m, respectively. Figure 16 shows the pressure comparison of the four best frequencies. When air cut off duration is 6 s, few differences are caused by pulse frequency when applying different air inflow time. When the frequency is 5 s–6 s, the peak pressure value reaches maximum, which is 8.45 m (rectangular nozzle on top of the pipe).

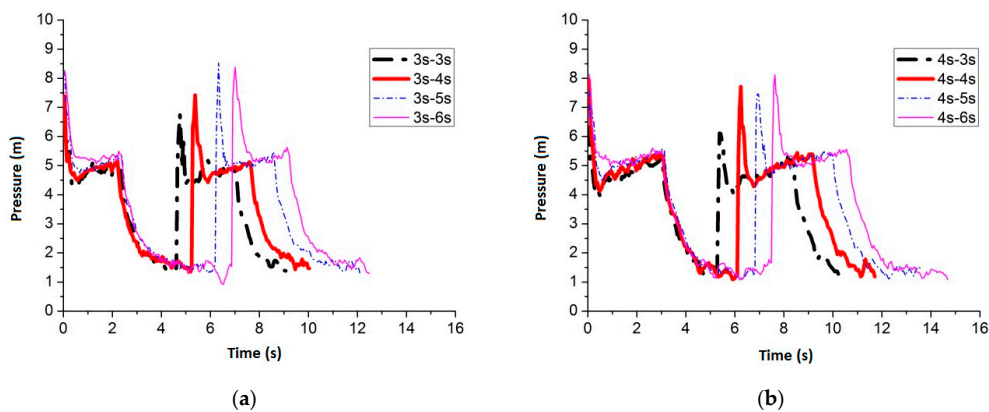


Figure 15. Cont.

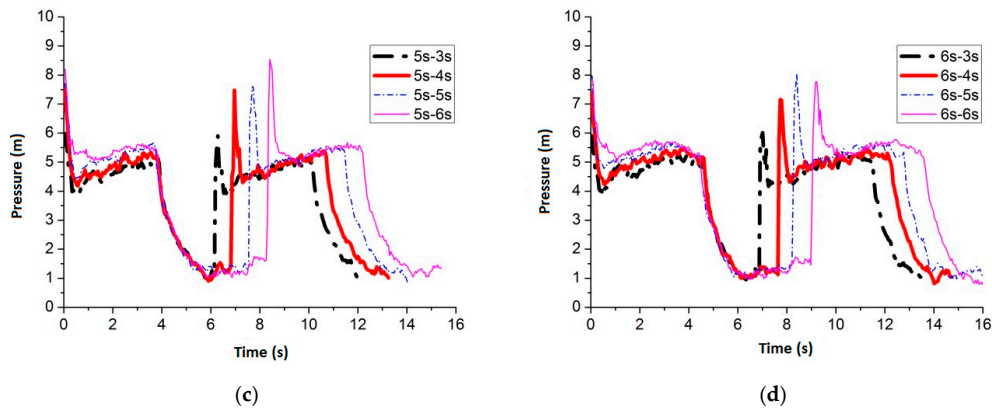


Figure 15. Pressure fluctuation of No. 1 sensing point (rectangular nozzle on top of the pipe): (a) air inflow time is 3 s; (b) air inflow time is 4 s; (c) air inflow time is 5 s; and (d) air inflow time is 6 s.

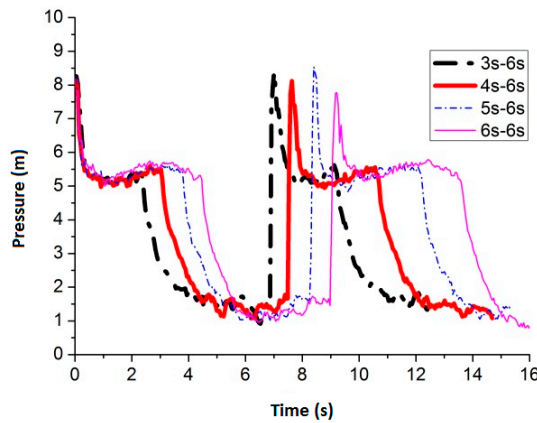


Figure 16. The four best pressure values (rectangular nozzle on top of the pipe).

The best frequency is not clear after air inflow is cut off for 6 s through the comparison of the four best frequencies (Figure 16). Therefore, four cycles of pressure data are selected to perform the statistical analysis in every operating condition to help find the best frequency (Table 6).

Table 6. Pressure values and statistical analysis after air inflow has been cut off for 6 s (rectangular nozzle on top of the pipe).

Frequency	Parameter	Average Peak Value (m)	Average Minimum Value (m)	Variation Range (m)	Average Value (m)	Peak Value Deviation
3 s–6 s		8.2548	0.9625	7.2923	3.2449	0.0955
4 s–6 s		8.1376	1.0338	7.1038	3.3550	0.1227
5 s–6 s		8.6996	0.9879	7.7118	3.4960	0.4364
6 s–6 s		7.9079	0.7558	7.1521	3.6445	0.1118

Figure 17 shows the average flow velocity of the water flow in the pipe by applying the above flushing conditions.

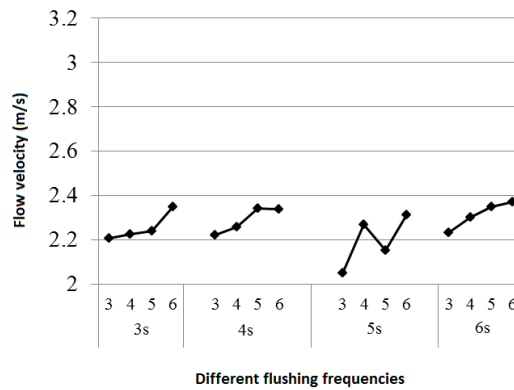


Figure 17. Flow velocity comparison of all the frequencies (rectangular nozzle on top of the pipe).

In Table 6 and Figure 17, the best frequency can be obtained as 5 s–6 s (rectangular nozzle on top of the pipe). The average water flow velocity reaches 2.314 m/s in the pipe at the frequency 5 s–6 s, and the average peak pressure value and the fluctuation range reach maximum simultaneously.

Nozzle at the Bottom of the Pipe

Figure 18 shows the maximum average peak pressure comes after air inflow is cut off for 6 s by setting the air inflow time invariant. When the frequency is 3 s–6 s, 4 s–6 s, 5 s–6 s and 6 s–6 s, the average peak pressure is 8.32 m, 8.21 m, 7.83 m and 8.03 m, respectively. Figure 19 shows the pressure comparison of the four best frequencies. When air cut off duration is 6 s, few differences are caused by pulse frequency when different air inflow time is applied. When the frequency is 3 s–6 s, the peak pressure reaches maximum, which is 8.32 m (rectangular nozzle at the bottom of the pipe).

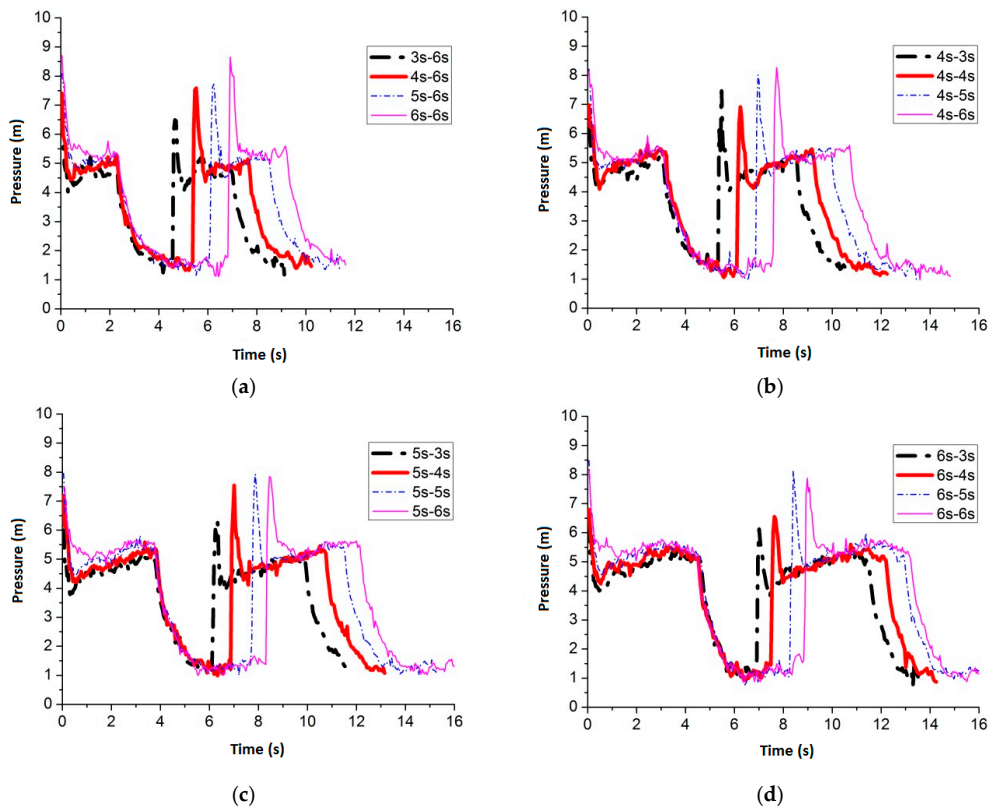


Figure 18. Pressure fluctuation of No. 1 sensing point (rectangular nozzle at the bottom of the pipe): (a) air inflow time is 3 s; (b) air inflow time is 4 s; (c) air inflow time is 5 s; and (d) air inflow time is 6 s.

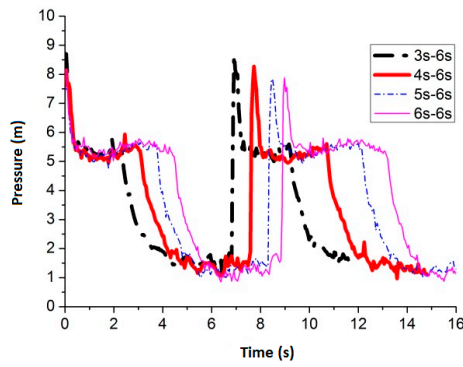


Figure 19. The four best pressure values (rectangular nozzle at the bottom of the pipe).

The best frequency is not clear after air inflow is cut off for 6 s through the comparison of the four best frequencies (Figure 19). Therefore, four cycles of pressure data are selected to perform the statistical analysis in every operating condition to help to find the best frequency (Table 7).

Table 7. Pressure values and analysis after air inflow has been cut off for 6 s (rectangular nozzle at the bottom of the pipe).

Frequency	Parameter	Average Peak Value (m)	Average Minimum Value (m)	Variation Range (m)	Average Value (m)	Peak Value Deviation
3 s–6 s		8.5594	1.0833	7.4761	3.2360	0.1221
4 s–6 s		8.1811	1.0471	7.1340	3.3390	0.1269
5 s–6 s		7.9973	0.9794	7.0179	3.4948	0.2000
6 s–6 s		8.0312	0.8706	7.1606	3.6354	0.1027

Figure 20 shows the average flow velocity of the water flow in the pipe by applying the above flushing conditions.

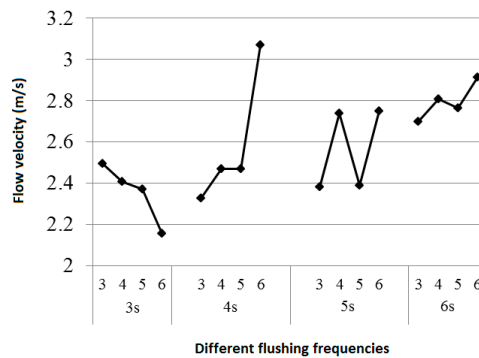


Figure 20. Flow velocity comparison of all the frequencies (rectangular nozzle at the bottom of the pipe).

In Table 7 and Figure 20, the average peak pressure value and the fluctuation range of No. 1 sensing point reach maximum simultaneously at the frequency 3 s–6 s (rectangular nozzle at the bottom of the pipe). However, the average water flow velocity is low, which is 2.154 m/s in the pipe at the frequency 3 s–6 s. Therefore, 6 s–6 s is considered as the best frequency, and at this frequency the flow velocity in the pipe is 2.912 m/s.

Comparison of Nozzle Locations

At the best flushing frequencies, setting different nozzle locations, the fluctuation ranges and the flow velocity of No. 1 sensing point are compared and given in Table 8. Setting the rectangular nozzle at the bottom of the pipe, the average flow velocity reaches maximum, and the peak pressure value

deviation reaches minimum. However, setting the rectangular nozzle in the middle or on top of the pipe, the peak pressure value and the fluctuation range are high, as well as the deviation, especially the variance of the average peak pressure value reaches 0.4364 when the rectangular nozzle is set on top of the pipe. The above results indicate that the flow velocity and pressure fluctuation range are high and steady when the rectangular nozzle is set in the middle of the pipe. The best frequencies for pipe flushing are between 5 s–6 s and 6 s–6 s. The best air inflow frequency not only ensures enough air inflow amount for keeping the ejection flow flushing, but also avoids the negative effects on the flushing results by over air inflow amount. Similarly, in summary, two-phase (gas and water) high energy flushing effect on the internal pipe wall can be secured at the best air inflow frequencies.

Table 8. Flushing results by setting rectangular nozzle at different locations.

Location \ Parameter	Average Peak Value (m)	Average Minimum Value (m)	Variation Range (m)	Average Value (m)	Peak Value Deviation	Flow Velocity (m/s)
Top (5 s–6 s)	8.6996	0.9879	7.7118	3.4960	0.4364	2.314
Middle (6 s–6 s)	8.4591	0.8235	7.6356	3.6207	0.1342	2.447
Bottom (6 s–6 s)	8.0312	0.8706	7.1606	3.6354	0.1027	2.912

2.3.3. Slot Nozzle

Nozzle in the Middle of the Pipe

Figure 21 shows the maximum average peak pressure comes after air inflow is cut off for 6 s by setting the air inflow time invariant. When the frequency is 3 s–6 s, 4 s–6 s, 5 s–6 s and 6 s–6 s, the average peak pressure value is 7.68 m, 7.81 m, 7.52 m and 7.34 m, respectively. Figure 22 shows the pressure comparison of the four best frequencies. When air cut off duration is 6 s, few differences are caused by pulse frequency when different air inflow time is applied. At the frequency 4 s–6 s, the peak pressure reaches maximum, which is 7.81 m, by setting the slot nozzle in the middle of the pipe.

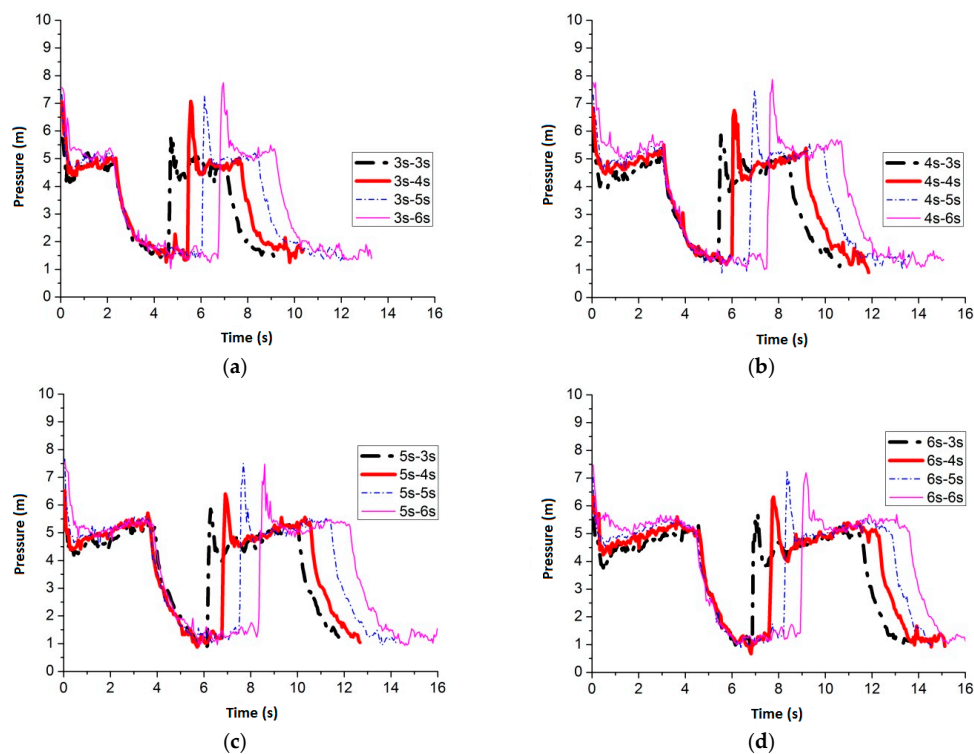


Figure 21. Pressure fluctuation of No. 1 sensing point when slot nozzle is set in the middle of the pipe (a) air inflow time is 3 s; (b) air inflow time is 4 s; (c) air inflow time is 5 s; and (d) air inflow time is 6 s.

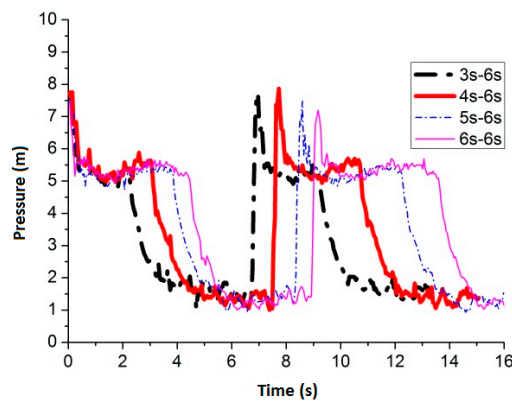


Figure 22. The four best pressure values when the slot nozzle is set in the middle of the pipe.

The best frequency is not clear after air inflow is cut off for 6 s through the comparison of the four best frequencies in Figure 22. Therefore, four cycles of pressure data are selected to perform the statistical analysis in every operating condition to help find the best frequency. The results are given in Table 9.

Table 9. Pressure values and statistical analysis after air inflow has been cut off for 6 s when the slot nozzle is set in the middle of the pipe.

Frequency	Parameter	Average Peak Value (m)	Average Minimum Value (m)	Variation Range (m)	Average Value (m)	Peak Value Deviation
3 s–6 s		7.6226	1.0362	6.5864	3.1815	0.0610
4 s–6 s		7.7085	0.9806	6.7278	3.3761	0.1064
5 s–6 s		7.5513	0.9492	6.6021	3.4420	0.0604
6 s–6 s		7.6311	0.8356	6.7955	3.5916	0.1245

Figure 23 shows the average flow velocity of the water flow in the pipe by applying the above flushing conditions.

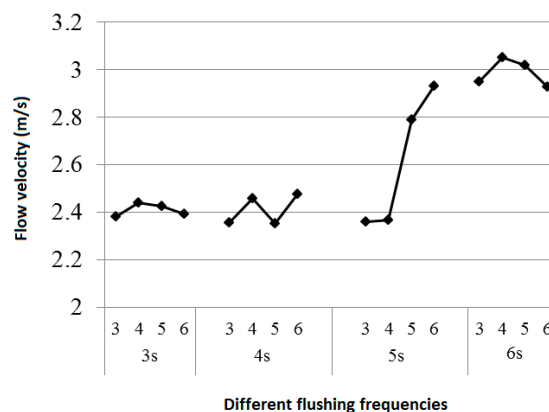


Figure 23. Flow velocity comparison of all the frequencies when the slot nozzle is set in the middle of the pipe.

In Table 9 and Figure 23, the pressure fluctuation range of No. 1 sensing point reaches maximum at the frequency 6 s–6 s when the slot nozzle is set in the middle of the pipe. The average water flow velocity reaches a high value which is 2.928 m/s in the pipe at the frequency 6 s–6 s. Therefore, 6 s–6 s is considered as the best frequency.

Nozzle on Top of the Pipe

Figure 24 shows the maximum average peak pressure comes after air inflow is cut off for 6 s by setting the air inflow time invariant. When the frequency is 3 s–6 s, 4 s–6 s, 5 s–6 s and 6 s–6 s, the average peak pressure is 7.51 m, 7.44 m, 6.99 m and 7.47 m, respectively. Figure 25 shows the pressure comparison of the four best frequencies. When air cut off duration is 6 s, few differences are caused by pulse frequency by applying different air inflow time. When the frequency is 3 s–6 s, the peak pressure reaches maximum, which is 7.51 m, when the slot nozzle is set on top of the pipe.

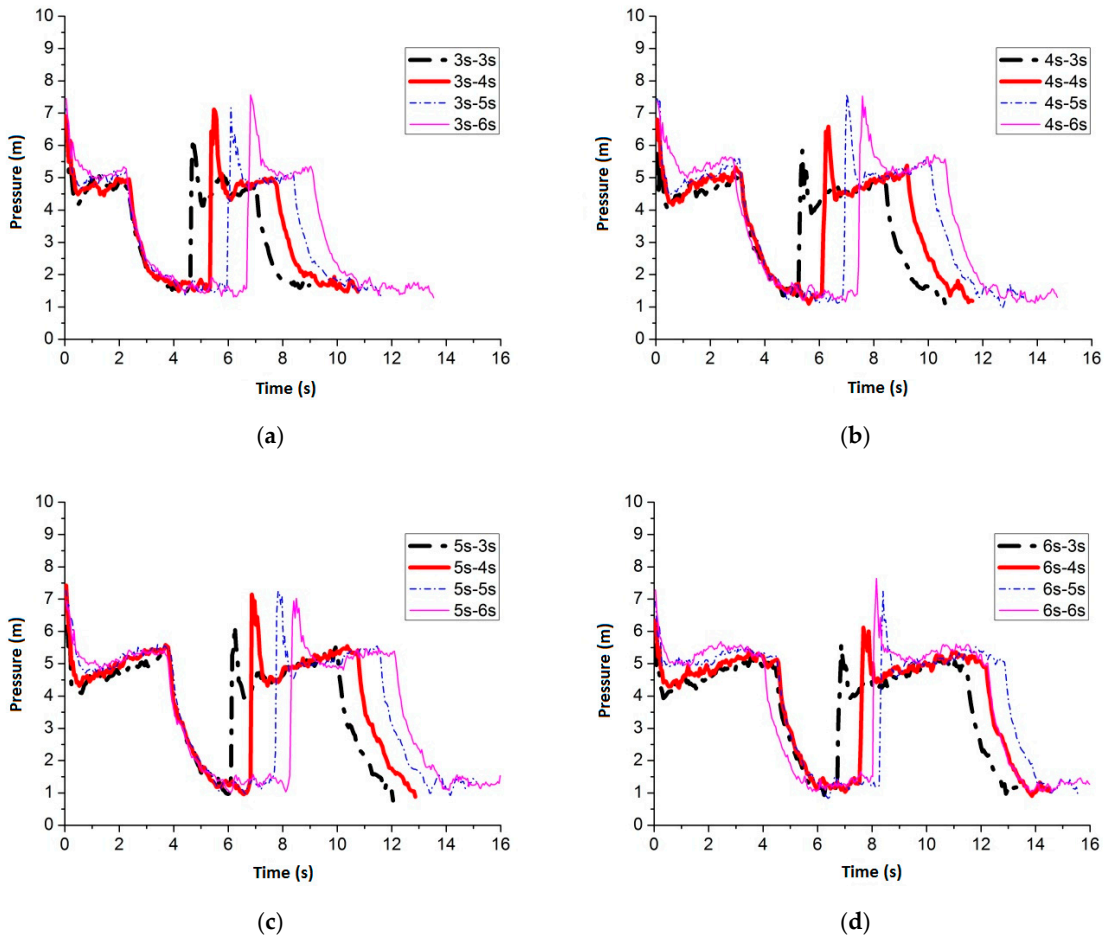


Figure 24. Pressure fluctuation of No. 1 sensing point when the slot nozzle is set on top of the pipe (a) air inflow time is 3 s; (b) air inflow time is 4 s; (c) air inflow time is 5 s; and (d) air inflow time is 6 s.

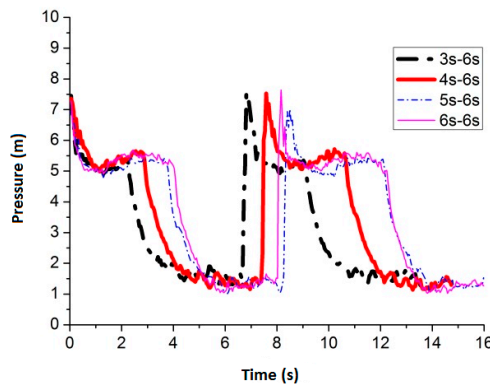


Figure 25. The four best pressure values when the slot nozzle is set on top of the pipe.

The best frequency is not clear after air inflow is cut off for 6 s through the comparison of the four best frequencies in Figure 25. Therefore, four cycles of pressure data are selected to perform the statistical analysis in every operating condition to help find the best frequency. The results are given in Table 10.

Table 10. Pressure values and statistical analysis after air inflow has been cut off for 6 s when the slot nozzle is set on top of the pipe.

Frequency	Parameter	Average Peak Value (m)	Average Minimum Value (m)	Variation Range (m)	Average Value (m)	Peak Value Deviation
3 s–6 s		7.7121	1.3021	6.4100	3.1782	0.3137
4 s–6 s		7.8184	0.9842	6.8342	3.3658	0.3693
5 s–6 s		7.2866	0.9516	6.3350	3.4161	0.1366
6 s–6 s		7.3132	0.9516	6.3616	3.5605	0.1650

Figure 26 shows the average flow velocity of the water flow in the pipe when the above flushing conditions are applied.

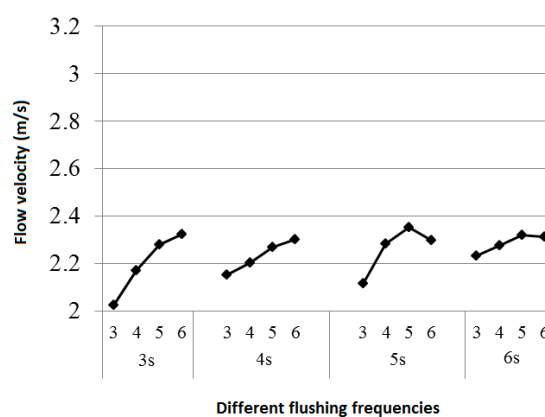


Figure 26. Flow velocity comparison of all the frequencies when the slot nozzle is on top of the pipe.

In Table 10 and Figure 26, the peak pressure and the pressure fluctuation range of No. 1 sensing point reach maximum simultaneously at the frequency 4 s–6 s when the slot nozzle is set on top of the pipe. The average water flow velocity reaches a high value which is 2.928 m/s in the pipe at the frequency 4 s–6 s. Therefore, 4 s–6 s is considered as the best frequency.

Nozzle at the Bottom of the Pipe

Figure 27 shows the maximum average peak pressure comes after air inflow is cut off for 6 s by applying invariant air inflow time. When the frequency is 3 s–6 s, 4 s–6 s, 5 s–6 s and 6 s–6 s, the average peak pressure is 7.71 m, 7.99 m, 8.07 m and 7.72 m, respectively. Figure 28 shows the pressure comparison of the four best frequencies. When air cut off duration is 6 s, there are few differences caused by pulse frequency when different air inflow time is applied. When the frequency is 5 s–6 s, the peak pressure reaches maximum, which is 8.07 m, when the slot nozzle is set at the bottom of the pipe.

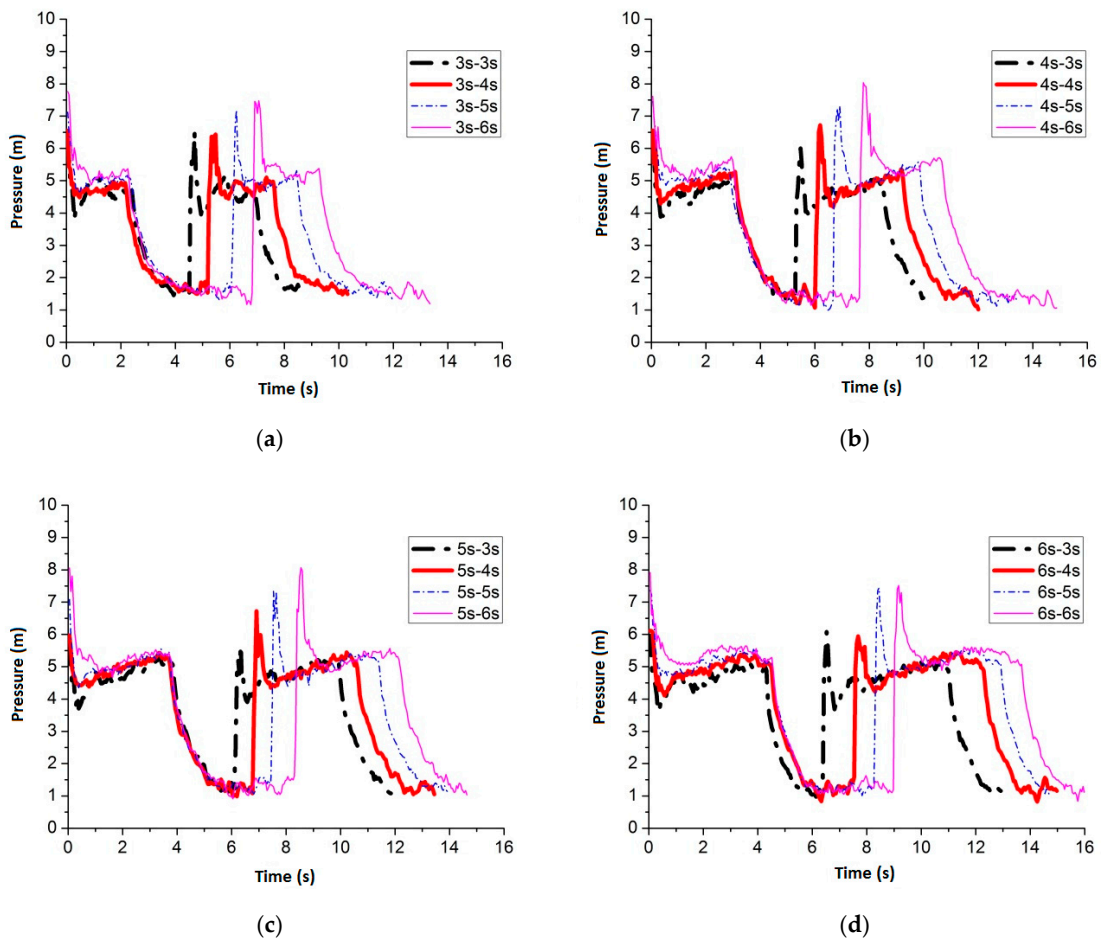


Figure 27. Pressure fluctuation of No. 1 sensing point when slot nozzle is set at the bottom of the pipe (a) air inflow time is 3 s; (b) air inflow time is 4 s; (c) air inflow time is 5 s; and (d) air inflow time is 6 s.

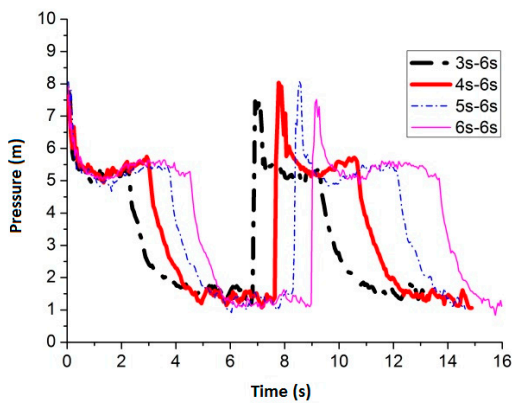


Figure 28. The four best pressure values when the slot nozzle is set at the bottom of the pipe.

The best frequency is not clear after air inflow is cut off for 6 s through the comparison of the four best frequencies in Figure 28. Therefore, four cycles of pressure data are selected to perform the statistical analysis in every operating condition to help find the best frequency. The results are given in Table 11.

Table 11. Pressure values and statistical analysis after air inflow has been cut off for 6 s when the slot nozzle is set at the bottom of the pipe.

Parameter Frequency	Average Peak Value (m)	Average Minimum Value (m)	Variation Range (m)	Average Value (m)	Peak Value Deviation
3 s–6 s	7.7894	1.0326	6.7569	3.1755	0.0985
4 s–6 s	7.8789	1.0604	6.8185	3.3937	0.1324
5 s–6 s	7.9744	0.9709	7.0034	3.4223	0.0919
6 s–6 s	7.5610	0.9359	6.6251	3.5801	0.1910

Figure 29 shows the average flow velocity of the water flow in the pipe when the above flushing conditions are applied.

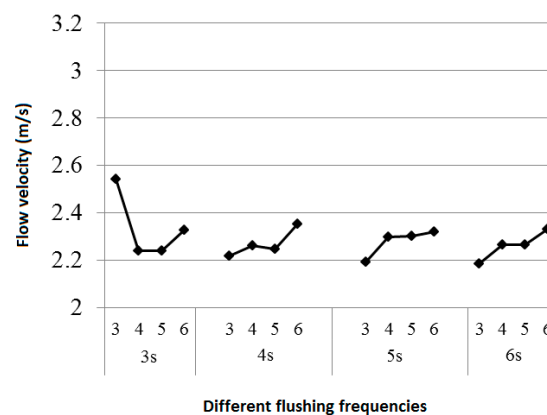


Figure 29. Flow velocity comparison of all frequencies when the slot nozzle is set at the bottom of the pipe.

In Table 11 and Figure 29, the best frequency can be obtained as 5 s–6 s when the slot nozzle is set at the bottom of the pipe. The average water flow velocity reaches 2.320 m/s in the pipe at the frequency 5 s–6 s, and the average peak value and the fluctuation range reach maximum simultaneously.

Comparison of Nozzle Locations

At the best flushing frequencies, setting different nozzle locations, the fluctuation range and the flow velocity of No. 1 sensing point are compared and given in Table 12. When the slot nozzle is set in the middle of the pipe, the average flow velocity reaches maximum, the peak value deviation is low, and the fluctuation range is high. The above results indicate that nozzle in the middle of the pipe is the best and most reliable for pipe flushing at the best frequencies when three different nozzle locations are set. The best frequencies are between 4 s–6 s and 6 s–6 s. The best air inflow frequency not only ensures enough air inflow amount for keeping the ejection flow flushing, but also avoids the negative effects on the flushing results by over air inflow amount. Similarly, in summary, two-phase (gas and water) high energy flushing effect on the internal pipe wall can be secured at the best air inflow frequencies.

Table 12. Flushing results when the slot nozzle is set at different locations.

Parameter Location	Average Peak Value (m)	Average Minimum Value (m)	Variation Range (m)	Average Value (m)	Peak Value Deviation	Flow Velocity (m/s)
Top (4 s–6 s)	7.8184	0.9842	6.8342	3.3658	0.3693	2.303
Middle (6 s–6 s)	7.6311	0.8356	6.7955	3.5916	0.1245	2.928
Bottom (5 s–6 s)	7.9744	0.9709	7.0034	3.4223	0.0919	2.320

2.3.4. Discussions on Nozzle Shapes

The effects of different nozzle locations based on the same shape of the air inflow nozzle have been compared and discussed in previous subsections. In this subsection, the effects of different nozzle shapes when they are set at the same locations will be compared and discussed. The best nozzle shape for every air inflow location will be selected.

At the best flushing frequencies, the fluctuation range and the flow velocity of No. 1 sensing point when different shape nozzles are set in the middle of the pipe are compared and given in Table 13. When the nozzle shape is slot, the flow velocity is the highest, but the pressure fluctuation range of the No. 1 sensing point is the lowest. When the nozzle shape is round, the pressure fluctuation range and average peak pressure value are both the highest, and the flow velocity is high. Therefore, the best flushing condition combination is to use the round nozzle and set it in the middle of the pipe operating at the frequency 5 s–6 s.

Table 13. Flushing results when different shape nozzles are set in the middle of the pipe.

Location \ Parameter	Average Peak Value (m)	Average Minimum Value (m)	Variation Range (m)	Average Value (m)	Peak Value Deviation	Flow Velocity (m/s)
Round (5 s–6 s)	8.7165	0.7111	8.0055	3.5498	0.2466	2.534
Rectangular (6 s–6 s)	8.4591	0.8235	7.6356	3.6207	0.1342	2.447
Slot (6 s–6 s)	7.6311	0.8356	6.7955	3.5916	0.1245	2.928

At the best flushing frequencies, the fluctuation range and the flow velocity of No. 1 sensing point when different shape nozzles are set on top of the pipe are compared and given in Table 14. Different shapes have little influence on the flow velocity. When the rectangular shape is used, the average peak and bottom pressure and the pressure fluctuation range simultaneously maximised. Therefore, the best flushing condition combination is to set the rectangular nozzle on top of the pipe operating at the frequency 5 s–6 s.

Table 14. Flushing results when different shape nozzles are set on top of the pipe.

Location \ Parameter	Average Peak Value (m)	Average Minimum Value (m)	Variation Range (m)	Average Value (m)	Peak Value Deviation	Flow Velocity (m/s)
Round (4 s–6 s)	8.6875	1.0217	7.6658	3.3755	0.2635	2.311
Rectangular (5 s–6 s)	8.6996	0.9879	7.7118	3.4960	0.4364	2.314
Slot (4 s–6 s)	7.8184	0.9842	6.8342	3.3658	0.3693	2.303

At the best flushing frequencies, the fluctuation range and the flow velocity of No. 1 sensing point when different shape nozzles are set at the bottom of the pipe are compared, as shown in Table 15. The frequency 5 s–6 s is considered as the best frequency because the flow velocity, average pressure peak value and the pressure fluctuation range reaches maximum simultaneously.

Table 15. Flushing results when different shape nozzles are set at the bottom of the pipe.

Location \ Parameter	Average Peak Value (m)	Average Minimum Value (m)	Variation Range (m)	Average Value (m)	Peak Value Deviation	Flow Velocity (m/s)
Round (4 s–6 s)	8.9498	1.0193	7.9305	3.4144	0.1342	2.957
Rectangular (6 s–6 s)	8.0312	0.8706	7.1606	3.6354	0.1027	2.912
Slot (5 s–6 s)	7.9744	0.9709	7.0034	3.4223	0.0919	2.320

Through the analysis and comparison in Tables 13–15 and the previous subsections, the best nozzle shape for every air inflow location and the best operating frequency are selected to achieve the best flushing result: a round air inflow nozzle at the bottom of the pipe operating at the frequency 4 s–6 s.

3. Case Study

3.1. Case Project Overview

This project is to apply flushing for the pipeline of the outer ring road of a city in Yangtze River Delta. It is a flushing work for a new pipeline before it is synchronised in the water distribution network. The pipe is connected by a T type rubber ring socket connector and its material is nodular cast iron. The lining is cement plaster for anticorrosion. The length of the pipeline is 891 m, and the diameter is DN1400 mm. The source water for flushing is from a DN1400 mm clean water pipe which is in parallel with the objective pipeline, and the DN1400 mm is a main transmission pipeline in the water network. To ensure the water demand of the downstream customers, flushing cannot use too much water amount. There is a crossover duct at 200 m distance from the pipe beginning. It is 14 m above the ground and its length is approximately 90 m. The other pipelines are in one approximately horizontal line. The drain pipe consists of two parts. The flushing pipe is connected with the DN800 mm drain pipe. There is a DN800 mm butterfly valve on the DN800 mm drain pipe. The butterfly valve is connected with a concentric reducer (DN800 × DN600). Then, through DN600 mm pipe, the waste water drains to the river.

3.2. Flushing Strategy

The flushing equipment for this case project consists of a pulse flushing generation system, a pulse control system and a visible monitoring system by using internet access. The visible monitoring system is deployed at the end of the flushing pipeline to monitor the sensory index of the flushing water quality and the results of the flushing in real time. The flushing frequencies can be controlled by the control panel to optimise the results of the flushing at any time. The monitoring devices include flow meter, portable turbidimeter and portable total chlorine tester for measuring the flow rate, turbidity and total chlorine of the end water. The water consumption for flushing is measured by recording the flow rate. The turbidity of the end water is recorded every 10 min. When the turbidity falls below 1 Nephelometric Turbidity Unit (NTU), the flushing process is stopped. The diagram of this project is shown in Figure 30.

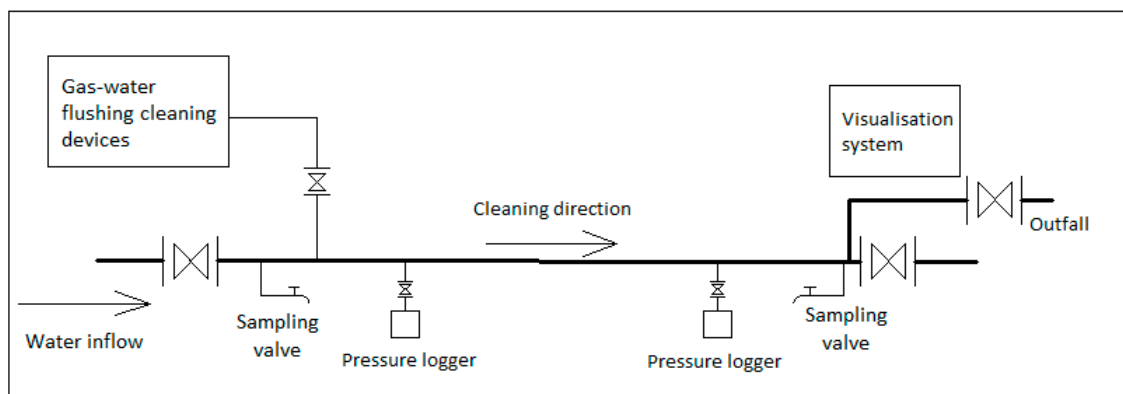


Figure 30. Diagram of the two-phase (gas and water) flushing process.

Based on the experimental results in Section 2, the best flushing condition combination is to set the round air inflow nozzle at the bottom of the pipe operating at the frequency 4 s–6 s. The results are verified by numerical modelling and experiments. Therefore, this case project uses these results. However, the experimental pipeline is acclinic but the pipeline used in this case project consists a bridge duct which is 14 m higher than the ground and its length is 200 m. The structure in this pipeline is more complex than the experimental one. Hence, based on the optimum combination, by using the

visualisation system at the end of the pipeline outfall to monitor the flushing results in real time and adjusting the frequencies at the beginning of the pipeline, the optimum flushing results are guaranteed.

3.3. Flushing Results

According to the “Code for construction and acceptance of water and sewerage pipeline works” (GB50268-2008) issued by the Ministry of Housing and Urban-Rural Development of the People’s Republic of China (MOHURD) and the General Administration of Quality Supervision [11], Inspection and Quarantine of the People’s Republic of China, the flushing for the water distribution pipelines should meet the following requirements. The flushing process should avoid the peak time of water consumption and be in succession. The first time of flushing should use clean water to flush until the turbidity of the end water is below 3 NTU. According to the “Standards for drinking water quality” (GB5749-2006) issued by the Ministry of Health of the People’s Republic of China and the Standardisation Administration of the People’s Republic of China [12], the conventional index of sanitiser and the requirements in drinking water are in Table 16.

Table 16. Conventional index of sanitiser and the requirements in drinking water.

Name of Disinfection	Reaction Time in the Water	Regulated Value from Treatment Plant	Minimum Value from Treatment Plant	Minimum Value at End Pipe
Chlorine and free chlorine preparation (free chlorine, mg/L)	At least 30 min	4	≥ 0.3	≥ 0.05

Figure 31 shows the data record of turbidity during the flushing process. At 14:05, flushing and air inflow commence. Before air inflow works, the turbidity of the pipe is 175.00 NTU (14.06). After air inflow works, the turbidity increases based on the results shown in the data record because of the separation of the internal pipe wall attachments and sediments to the water caused by flushing. It reaches the highest value 498.00 NTU at 14:16. With the continuous flushing, all the internal pipe wall attachments and sediments are separated to the water and discharged from the pipeline, and the turbidity starts to decrease. At 15:26, the turbidity is 0.85 NTU, which meets the requirements. Then, the air inflow is stopped and the flushing process is finished. The entire process lasts 1 h 20 min.

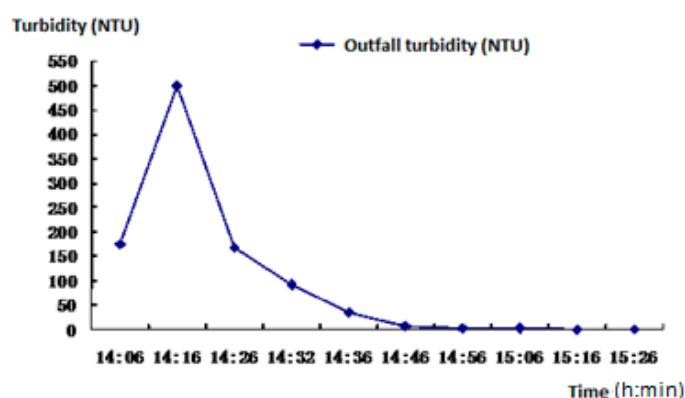


Figure 31. Data record of turbidity during the flushing cleaning process.

Figure 32 shows the data record of residual chlorine during the flushing process. At 14:05, water inflow starts and the initial residual chlorine concentration is 0.09 mg/L. At 14:06, air inflow starts and based on the results of the data record the residual chlorine in the pipeline starts to increase because the attachments and sediments from the internal pipe wall separate to the water and discharge outside the pipeline, which causes the decrease of inorganic substance and chlorine consumption. At 15:26, the residual chlorine concentration reaches 0.62 mg/L, which meets the requirements of the national code.

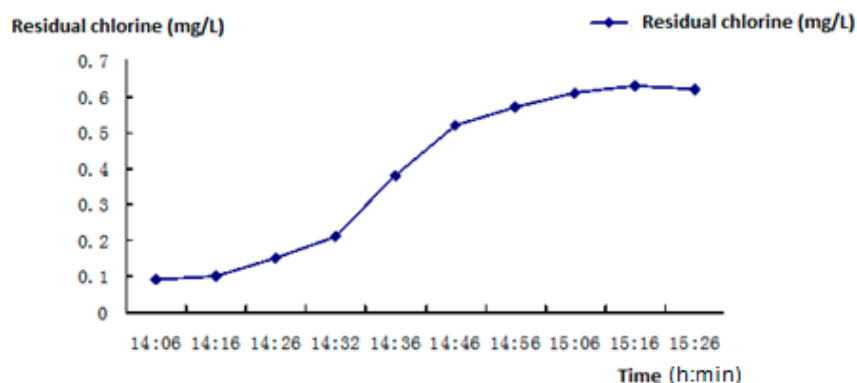


Figure 32. Data record of residual chlorine during the flushing process.

Figure 33 shows the photos inside the pipe before and after the flushing in this case study. The “growth-ring” is effectively removed by the flushing process.



Figure 33. Photos inside the pipe to show the flushing effect in this case study: (a) before flushing; and (b) after flushing.

For the DN1400 mm, 8 h are needed to reach the flushing target by using traditional single-phase flushing method. According to the national code [11], the flow velocity must be above 1.0 m/s when single-phase flushing method is used. Comparison of these two methods is given in Table 17.

Table 17. The comparison of two flushing methods in this case study.

Flushing Cleaning Method	Flushing Time	Water Consumption	Water Price	Total Cost
Single-phase flushing method	8 h	39,067 m ³	2.8 Yuan/m ³ (approximately 0.42 US dollars/m ³ or 0.36 Euros/m ³)	109,387.6 Yuan (approximately 16,421.9 US dollars or 14,096.5 Euro)
Two-phase (gas and water) flushing method	1 h 20 min	2000 m ³	2.8 Yuan/m ³ (approximately 0.42 US dollars/m ³ or 0.36 Euros/m ³)	5600 Yuan (approximately 840.7 US dollars or 721.7 Euros)

This case study is undertaken based on the experimental results obtained in the two-phase (gas and water) pulse flushing. To achieve the most effective, energy-saving and the least costly flushing target, the round air inflow nozzle is used and to set at the bottom of the pipe operating at the frequency 4 s–6 s. The results given in Table 17 show that the two-phase (gas and water) flushing method can save 95% of water and 6 h 40 min time against the single-phase flushing method, which is much more efficient and less costly.

4. Conclusions

An experimental framework is built for investigating the best setting combination of the two-phase (water and pressure) pulse flushing technology. The optimum setting combination of the two-phase pulse flushing method is obtained and verified by experimental results and subsequent discussions: a round air inflow nozzle at the bottom of the pipe operating at the frequency 4 s–6 s (air inflow time is 4 s and air cut off time is 6 s). A case project is introduced and through this project, the single-phase flushing method and the two-phase (gas and water) flushing method are compared and discussed. The two-phase flushing method can save 95% of water and 6 hours 40 min flushing time, which is much more efficient and less costly.

Acknowledgments: The authors appreciate the support from the colleagues in School of Municipal and Environmental Engineering, Harbin Institute of Technology.

Author Contributions: All the authors collaboratively conceived and carried out this research; M.Z. contributed experimental materials and laboratories; X.H. performed the experiments; Z.T. wrote the manuscript; W.W. critical revision of the manuscript and final approval to be published.

Conflicts of Interest: The authors declare no conflict of interest.

References

1. Machell, J.; Mounce, S.R.; Boxall, J.B. Online modelling of water distribution system: A UK case study. *Drink. Water Eng. Sci.* **2010**, *3*, 21–27. [CrossRef]
2. Ramos, H.; Loureiro, D.; Lopes, A.; Fernandes, C.; Covas, D.; Reis, L.F.; Cunha, M.C. Evaluation of chlorine decay in drinking water systems for different flow conditions: From theory to practice. *Water Resour. Manag.* **2010**, *24*, 815–834. [CrossRef]
3. Douterelo, I.; Husband, S.; Boxall, J.B. The bacteriological composition of biomass recovered by flushing an operational drinking water distribution system. *Water Res.* **2014**, *54*, 100–114. [CrossRef] [PubMed]
4. Zhao, H.B.; Li, X.; Zhao, M. The “growth-ring” of the water distribution pipeline. In *Hygiene in Water Distribution Pipeline*, 1st ed.; China Architecture & Building Press: Beijing, China, 2008.
5. Husband, P.S.; Boxall, J.B. Asset deterioration and discolouration in water distribution systems. *Water Res.* **2011**, *45*, 113–124. [CrossRef] [PubMed]
6. LeChevallier, M.W.; Babcock, T.M.; Lee, R.G. Examination and characterisation of distribution system biofilms. *Appl. Environ. Microbiol.* **1987**, *53*, 2714–2724. [PubMed]
7. Szewzyk, U.; Szewzyk, R.; Manz, W.; Schleifer, K.H. Microbiological safety of drinking water. *Annu. Rev. Microbiol.* **2000**, *54*, 81–127. [CrossRef] [PubMed]
8. Husband, P.S.; Boxall, J.B. Field studies of discolouration in water distribution systems: Model verification and practical implications. *J. Environ. Eng. ASCE* **2010**, *136*, 86–94. [CrossRef]
9. Teng, H.; Guan, Y.T.; Zhu, W.P. Effect of biofilm on cast iron pipe corrosion in drinking water distribution system: Corrosion scales characterisation and microbial community structure investigation. *Corros. Sci.* **2008**, *50*, 2816–2823. [CrossRef]
10. Li, S.; Zhang, X.J. The growth and development of the biological membrane on the water distribution pipe wall and their influence factors. *Water Supply Drain. China* **2003**, *19*, 49–52.
11. Jiao, Y.D. *Code for Construction and Acceptance of Water and Sewerage Pipeline Works (GB50268-2008)* by the Ministry of Housing and Urban-Rural Development of the People’s Republic of China (MOHURD) and the General Administration of Quality Supervision; China Architecture & Building Press: Beijing, China, 2009.
12. Jin, Y.L.; E, X.L.; Zhang, L. *Standards for Drinking Water Quality (GB5749-2006)* by the Ministry of Health of the People’s Republic of China and the Standardisation Administration of the People’s Republic of China; China Zhijian Publishing House Press: Beijing, China, 2007.

